

Research on Wheel Rail Wear for a 140 t Open Type Hot Metal Car

Bo Feng¹, Sumei Jia², Guosheng Feng^{2*}

¹HCIG Communication Investment Co. Ltd., Shijiazhuang, China

²School of Mechanical Engineering, Shijiazhuang Tiedao University, Shijiazhuang, China

Email: *fgs2005@126.com

How to cite this paper: Feng, B., Jia, S.M. and Feng, G.S. (2020) Research on Wheel Rail Wear for a 140 t Open Type Hot Metal Car. *Engineering*, 12, 563-580.
<https://doi.org/10.4236/eng.2020.128039>

Received: July 13, 2020

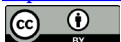
Accepted: August 16, 2020

Published: August 19, 2020

Copyright © 2020 by author(s) and Scientific Research Publishing Inc.

This work is licensed under the Creative Commons Attribution International License (CC BY 4.0).

<http://creativecommons.org/licenses/by/4.0/>



Open Access

Abstract

To maintain the safety of an open-type hot-metal car and to reduce wheel-rail wear during transportation, simulation models of the main components of such car were built using Pro/E software and then tested. In particular, the Pro/E models were imported into ADAMS/Rail for assembly and then used to construct a complete hot-metal car dynamic model. Locomotive wheel-rail attack angle, wheel-rail lateral force, and wear index were used as evaluation parameters during the simulation to analyze the effects of bogie parameter, rail parameter, and speed of the hot-metal car on wheel-rail wear. An improvement scheme for reducing wheel-rail wear was proposed based on the result of the dynamic simulation, wherein wheel-rail wear and curving performance were analyzed and compared. The simulation provided an important reference for evaluating and improving the dynamic performance of the hot-metal car. The applied effect showed that the improvement scheme is effective.

Keywords

Hot-Metal Car, ADAMS/Rail, Dynamic Simulation, Wheel and Rail Wear

1. Introduction

A hot-metal car is a special vehicle for transporting hot iron for iron works. With the rapid development of the steel industry, fundamental standards for hot-metal cars have been established in terms of safety, efficiency, and load capacity. Steel manufacturers aim to further develop hot-metal cars. The advantages of appropriate capacity, low cost, huge market demand, and technical difficulty have made hot-metal cars with the 140 t capacity the most competitive in

*Corresponding author.

the market. A hot-metal car has several limiting factors, such as its structure, the workshop building area of the steel manufacturer, the transport line, as well as the high temperature and liquid features of hot metal. These factors can cause numerous problems in transporting hot iron, such as low speed, heavy axle load, short interval distance without breakdown, bad curving performance, and bad wheel rim wear. In the example presented in this paper, the wear between the wheel and the rail has damaged a 140 t open hot-metal car, causing it to derail during transportation.

To solve these problems, V. P. Pipyuk and V. F. Polyakov *et al.* conducted research on the fluid dynamics of melting metal in a 350 t hot metal car using a numerical method [1]. A. G. Belkovskii and Ya. L. Kats proposed a mathematical model of temperature change in a hot-metal car while filling the car with red-hot semi-finished products [2]. Through analysis and comparison of the production efficiency and heat loss, D. N. Makarov *et al.* drew the conclusion that a 140 t hot-metal car outperforms a 100 t hot-metal car [3]. M. Ignesti *et al.* developed a wear model for predicting wheel-and-rail profile evolution in railway systems [4]. J. Pombo *et al.* studied the wear evaluation of railway wheels based on multi-body dynamics and wear computation [5]. A. A. Shabana *et al.* developed an elastic force model for wheel/rail contact problems [6]. E. Meli *et al.* determined wheel-rail contact points using semi-analytical methods and compared classical with neural network-based procedures [7] [8]. Xie Suming, Chang Liangwei, and other Chinese scholars researched the operation stability and curving performance of hot-metal cars using dynamic simulation software such as ADAMS/Rail and SIMPACK [9] [10] [11]. However, only a few scholars had investigated the wear of a three-axle bogie hot-metal car under special circumstances such as low speed, heavy load, small curve radius, and super-elevation. Using Pro/E and ADAMS/Rail, the authors of the present study conducted a dynamic simulation of a 140t open hot-metal car and analyzed its wear, which is associated with the relevant parameters of the car and the rail. The authors then proposed a low-wear solution, which provides references for evaluating and improving the performance of a hot-metal car.

2. Establishing the Complete Car Model

The 140 t open hot-metal car used in this study consisted of a hot-metal pot, a car frame, and two three-axle bogies, which differ from traditional bogies. This three-axle bogie (modified 110-G type) is made up of a side-frame suit and a swing bolster. The side-frame suit contains a universal two-axle bogie and an additional one-axle bogie, which are connected by a bolt. This design does not only guarantee sufficient strength but also cuts down raw material costs and makes part replacement convenient. The bogie design is shown in **Figure 1**.

The Pro/E models of all components were initially established according to the product drawing of the manufacturer. The car frame was used to sustain the load and transmit traction force while simultaneously serving as the fixing

foundation of the entire car. The car frame is shown in **Figure 2**. **Figure 3** illustrates the bogie system after importing the Pro/E model into ADAMS/Rail. **Figure 4** shows the complete dynamic model of the car. The technical parameters of the 140 t open hot-metal car are presented in **Table 1**.

The rationality of the model can be verified by comparing the calculated weight of the Pro/E model with the measured value on the computer-aided design drawings of the manufacturer. The wheel set, car frame, side frame, hot-metal pot, and axle box clearly have almost identical weights, as shown as in **Table 2**.

The bolster had a complex structure, thus, some of its parts were simplified, and weight errors were in a small extent of engineering acceptable. The car can carry 140 t of hot metal because iron slag may be present in the smelting hot iron, the density of which is 2300 kg/m^3 . However, iron slag content cannot be

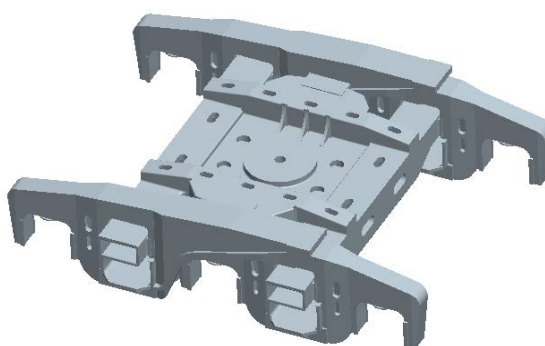


Figure 1. The bogie of the 140 t hot metal car.

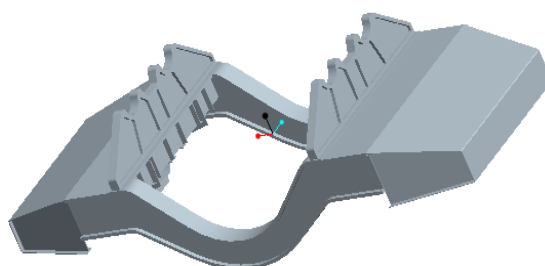


Figure 2. The frame of the 140 t hot metal car.

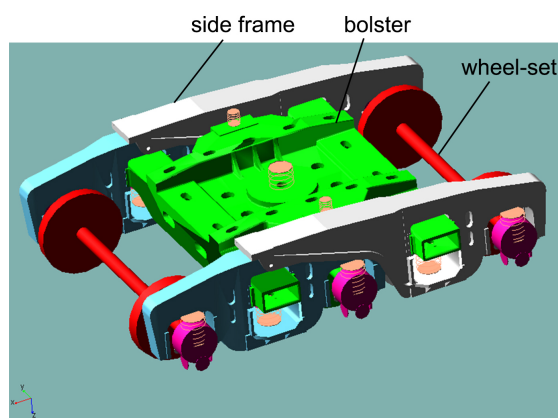


Figure 3. The bogie subsystem.

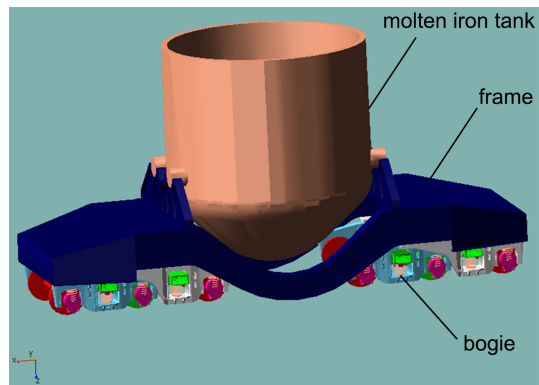


Figure 4. The dynamic model.

Table 1. The 140 t open hot metal car's technical parameters.

Parameters	Numerical value
Length of vehicle	9660 (mm)
Maximum height	4550 (mm)
Rigid wheel base	1300 (mm)
Distance between bogie centre	5380 (mm)
Distance between side frame	2040 (mm)
Distance between center plates	5380 (mm)
Distance between side bearing	1500 (mm)
Axial length	2250 (mm)
Diameter of wheel tread	650 (mm)
Mass of single round	0.993 (t)
Mass of body	187.15 (t)
Mass of bogie	9.056 (t)
Mass of frame	16.35 (t)
Capacity of hot-metal bottle	140 (t)
Gross weight of melted iron and pot	170 (t)
Axle load	34 (t)
Spring stiffness of bogie	12.06 (kN/mm)
Spring deflection of bogie	35 (mm)
Track gauge	1435 (mm)
Minimum radius of curvature	100 (m)
Maximum running speed	20 (km/h)

measured accurately. Based on a conservative calculation and assuming that the liquid level was 2.1 m high and its density was 7138 kg/m^3 , we estimated that the hot iron weight was 146 t, and that the distance between the gravity center of the hot iron and rail surface was 2.35 m. The rotational inertias of the main parts are shown in **Table 3**.

Table 2. Contrast of main parts basic parameters of hot-metal-car (kg).

Name of parts	Measured weight	Calculating weight
A wheel-set	993	996
Frame	16,350	16,250
Ladle (including firebrick)	30,000	29,500
Side frame 1	492	470
Side framer 2	1105	1080
Bolster	2610	2808
Molten iron	140,000	142,000

Table 3. Rotational inertias of main parts (kg·m²).

Parts name	X axis rotational inertia	Y axis rotational inertia	Z axis rotational inertia
Car body	321,500	408,600	406,800
Side frame	63	647	697
Swing bolster	845	678	1439
Wheel set	471	471	34

3. Effect of Bogie-Related Parameters on Wheel-Rail Wear

3.1. Friction Coefficients of the Center Plate and Side Bearing

Figure 5 shows the effects of the friction coefficients between the bogie center plate and the side bearings on wheel-rail wear in the multibody model. According to the actual operating state, the curve length of 300 m and operating speed of 15 km/h were defined as the baseline simulation case. Track irregularity was generally described by power spectrum density. Different values of the track spectrum could be obtained via field measurements of line conditions. The line conditions were divided into six levels.

The first level was the worst, whereas the sixth level was the best. The hot-metal car was operated in the manufacturing workshop, and the main influencing factor on track irregularity was wheel-rail wear. According to the actual measurements record, track spectrum level 5 was selected [12]. The center plate and side-bearing contact frame were directly determined to be partially worn. Friction coefficients were set as 0.4, 0.3, 0.2, and 0.1. The friction coefficient 0.2 was provided by the manufacturer. The other friction coefficients were used for simulation comparison. **Figure 6** shows that the curve of the wheel-rail wear changed with the friction coefficient of the center plate and side bearing. Increasing friction coefficient caused the wheel-rail creep forces and wear index to increase as well. In here [13],

$$W = F_x \varepsilon_x + F_y \varepsilon_y \quad (1)$$

W —wear index;

F_x —the longitudinal force of wheel-rail;

ε_x —the longitudinal creepage;

F_y —the lateral force of wheel-rail;

ε_y —the lateral creepage.

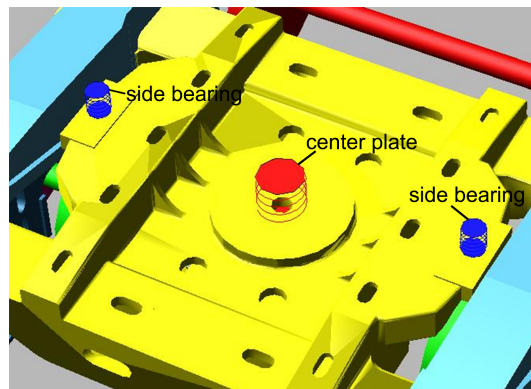


Figure 5. The center plate and side bearing.

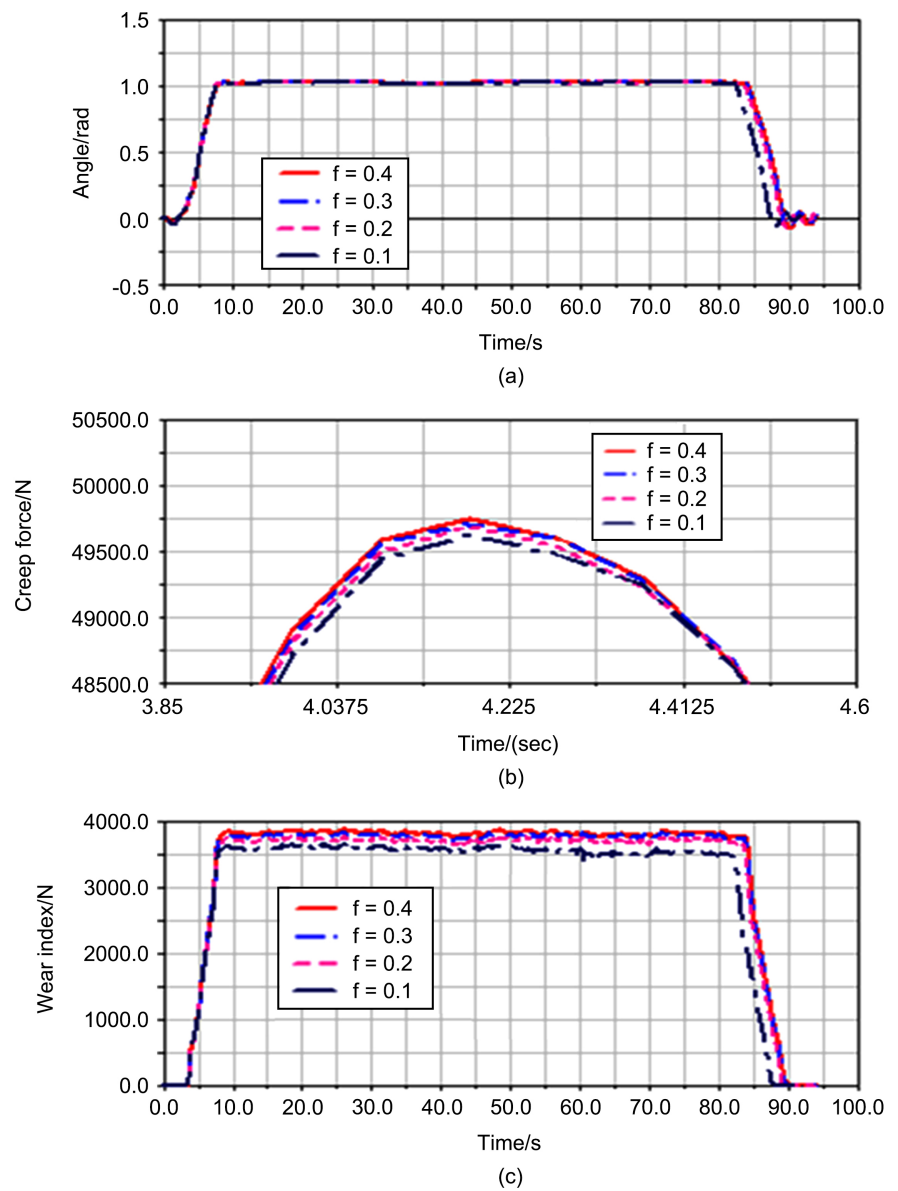


Figure 6. The effect of friction coefficient of center plate and side bearing on wheel-rail wear. (a) Wheel-rail attack angle; (b) Creep force; (c) Wheel-rail wear index.

3.2. Axle Box Positioning Size

The position of the axle box in the modified bogie can be determined by the guide frame. When the longitudinal clearance of the original car stop was set to 10 mm, the lateral clearances were set to 15 mm (condition 1), 10 mm (condition 2), and 5 mm (condition 3). When the lateral clearance was set to 10 mm, the longitudinal clearances were set to 15 mm (condition 4) and 5 mm (condition 5). The clearance of side frame guide is shown in **Table 4**.

Using the aforementioned parameters, the simulation of the effects of the longitudinal and lateral clearances between the side-frame box and guiding frame on wheel-rail wear was conducted. **Figure 7** shows that when the lateral clearance increased by 5 mm, the wear index of the guide wheel set decreased by 1.7%;

Table 4. Clearance of side frame guide.

Working condition	Lateral clearance (mm)	Longitudinal clearance (mm)
Working condition 1	15	10
Working condition 2	10	10
Working condition 3	5	10
Working condition 4	10	15
Working condition 5	10	5

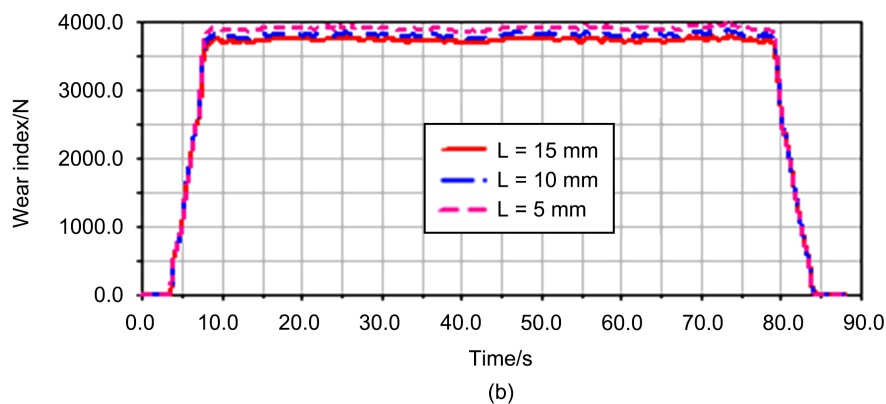
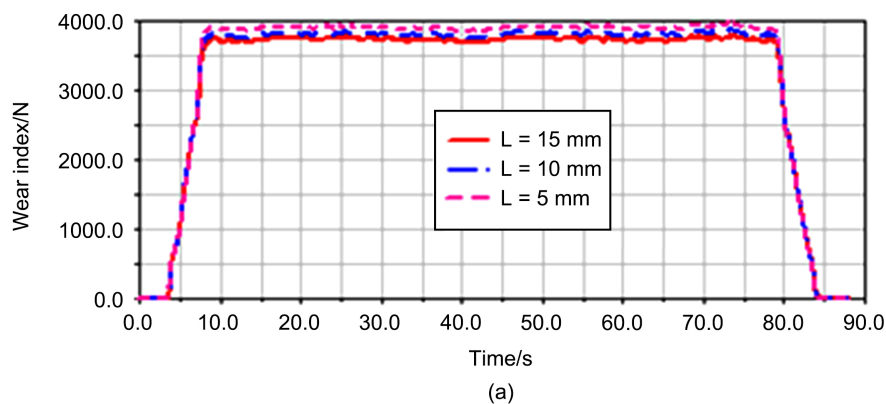


Figure 7. The effect of lateral clearance and longitudinal clearance on wheel-rail wear. (a) Wheel-rail wear index of lateral clearance; (b) Wheel-rail wear index of longitudinal clearance.

however, when the lateral clearance decreased by 5 mm, the wear index of the guide wheel set increased by 2.6%. When the longitudinal clearance increased by 5 mm, the wear index of the wheel set decreased by 10%, which is greater than the wear index when the longitudinal clearance decreased by 5 mm. The simulation results show that increasing the longitudinal and lateral clearances of the side-frame box is helpful in reducing the wheel-rail wear index and that the effect of longitudinal clearance on wheel-rail wear is greater than that of lateral clearance. Therefore, to satisfy the design requirements of the entire vehicle, increasing the position clearance appropriately will help reduce wheel-rail wear [13].

3.3. Vertical Stiffness of the Spring

The bogie spring device of the hot-metal car is responsible for reducing vehicle vibration and impact caused by uneven lines, wheel scratches, and elliptical wheels. Therefore, selecting the appropriate spring stiffness can effectively reduce the interaction between the wheel and the rail, improve the stability of vehicle operation, guarantee the safety of goods during transportation, and extend the life of the vehicle. Three spring stiffness values due to constructive criteria, namely, 10, 12, and 14 kN/mm, were selected for the simulation. The spring stiffness of 12 kN/mm was an approximate value of 12.06 kN/mm that was provided by the manufacturer. The spring stiffness values of 10 kN/mm and 14 kN/mm were used for comparison. **Figure 8** shows that the curve of wheel-rail wear changed with spring stiffness value.

The simulation results show that wheel-rail lateral force, wheel-set attack angle, and wheel-rail wear exhibited a negligible increase with the increase in the vertical stiffness of the spring. That is, changes in vertical stiffness have minimal effect on wheel-rail wear.

4. Effects of Orbital Parameters on Wheel-Rail Wear

Hot-metal cars used in the metallurgical industry mainly travel between the blast furnace and steel-making furnace. Such cars have a short running distance, low speed, and huge loading capacity; however, they lack a standard track design compared with railway freight trains. This limitation significantly affects the safety of hot-metal transportation. Therefore, the effects of orbital parameters on wheel-rail wear must be investigated.

4.1. Length of Transition Curve

In the dynamic analysis of the hot-metal car, various indices exhibited a sudden increase at the junction of the transition and circular curves because the vehicle there were impact between the wheels of the vehicle and the rail, which seriously affected the curving performance of the hot-metal car and threatened the safety of hot-metal transportation. To analyze the effect of different lengths of transition curve on wheel-rail impact, the lengths of 20, 30, and 40 m were set as conditions 1, 2, and 3, respectively.

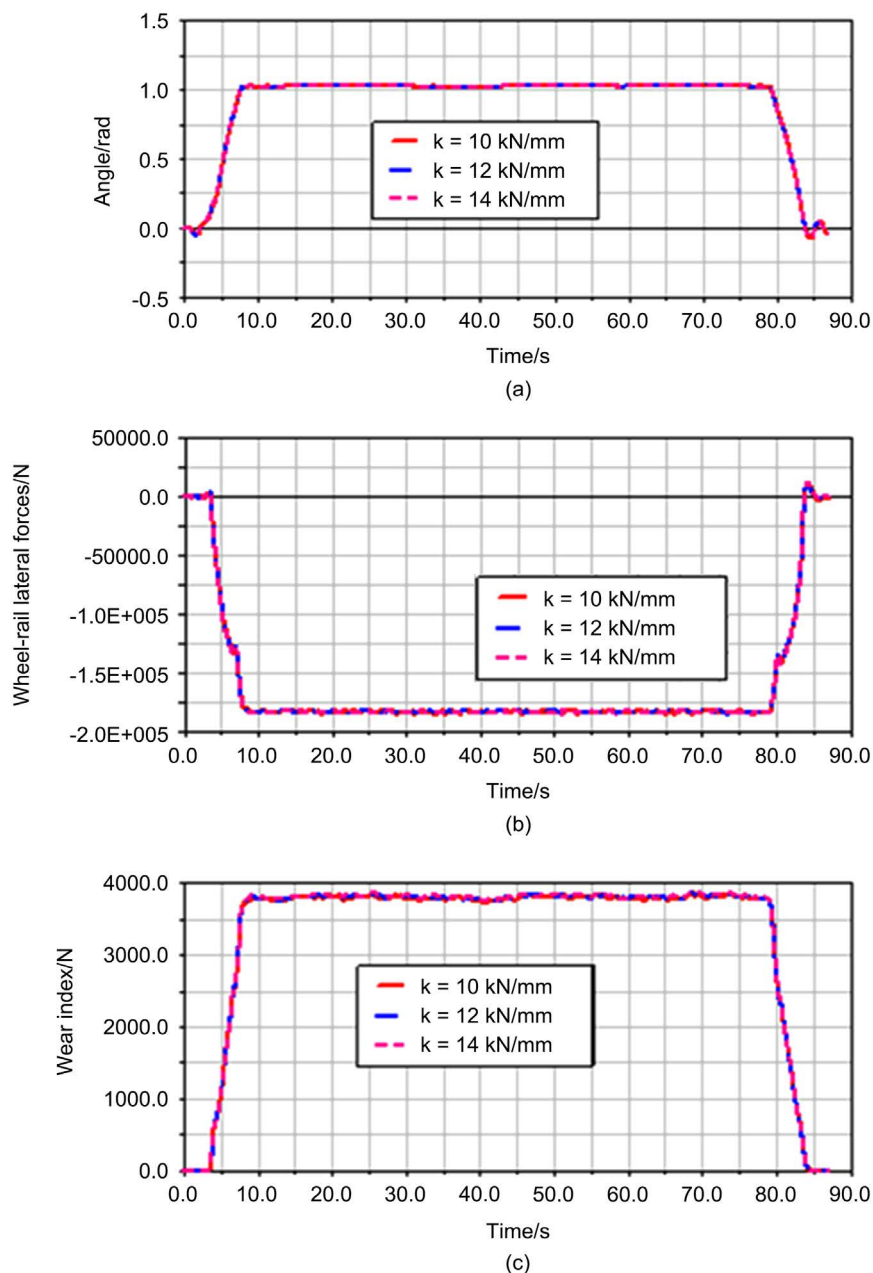


Figure 8. The effect of spring stiffness on wheel-rail wear. (a) Wheel-rail attack angle; (b) Wheel-rail lateral force; (c) Wheel-rail wear index.

Figure 9 shows that the effect of extending the transition curve on the wheel-rail attack angle was minimal. In addition, the maximum wheel-rail lateral force did not evidently change. However, lateral wheel-rail forces gradually decreased at the junction of the transition and circular curves. Moreover, the effect on the vehicle system gradually weakened. Such finding is consistent with the results of theoretical deduction [14]. With a longer transition curve, the maximum of the wheel-rail wear index decreased and the amplitude of vibration decreased, however these effects are smaller. Thus, extending the transition curve is beneficial in reducing wheel-rail impact; however, its effect on wheel-rail wear remains unclear.

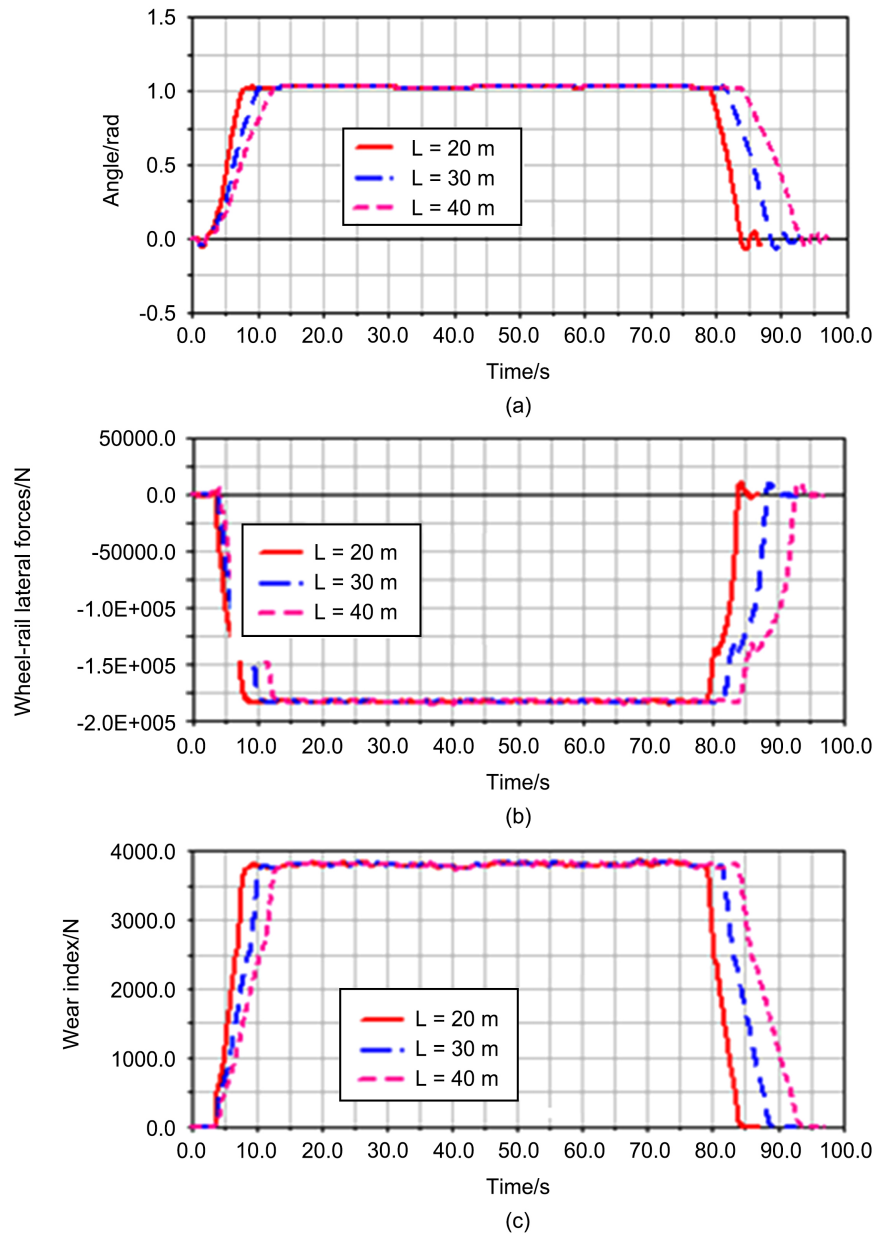


Figure 9. The effect of transition curve on wheel-rail wear. (a) Wheel-rail attack angle; (b) Wheel-rail lateral force; (c) Wheel-rail wear index.

4.2. Curve Radius

As the main geometric parameter of a curve, curve radius has a decisive effect on vehicle curving performance. The curve radius of the running line of the hot-metal car is limited, thus, the curve radii of 100, 150, and 200 m were respectively set as conditions 1, 2, and 3 to analyze the effect of different curve radius on wheel-rail wear. **Figure 10** shows that as the curve radius increased from 100 m to 150 m, the wheel-rail attack angle decreased to nearly half of the primitive value, and the wheel-rail wear index evidently decreased by 62.5%. As the curve radius increased from 150 m to 200 m, the rate of overall wear slowed down.

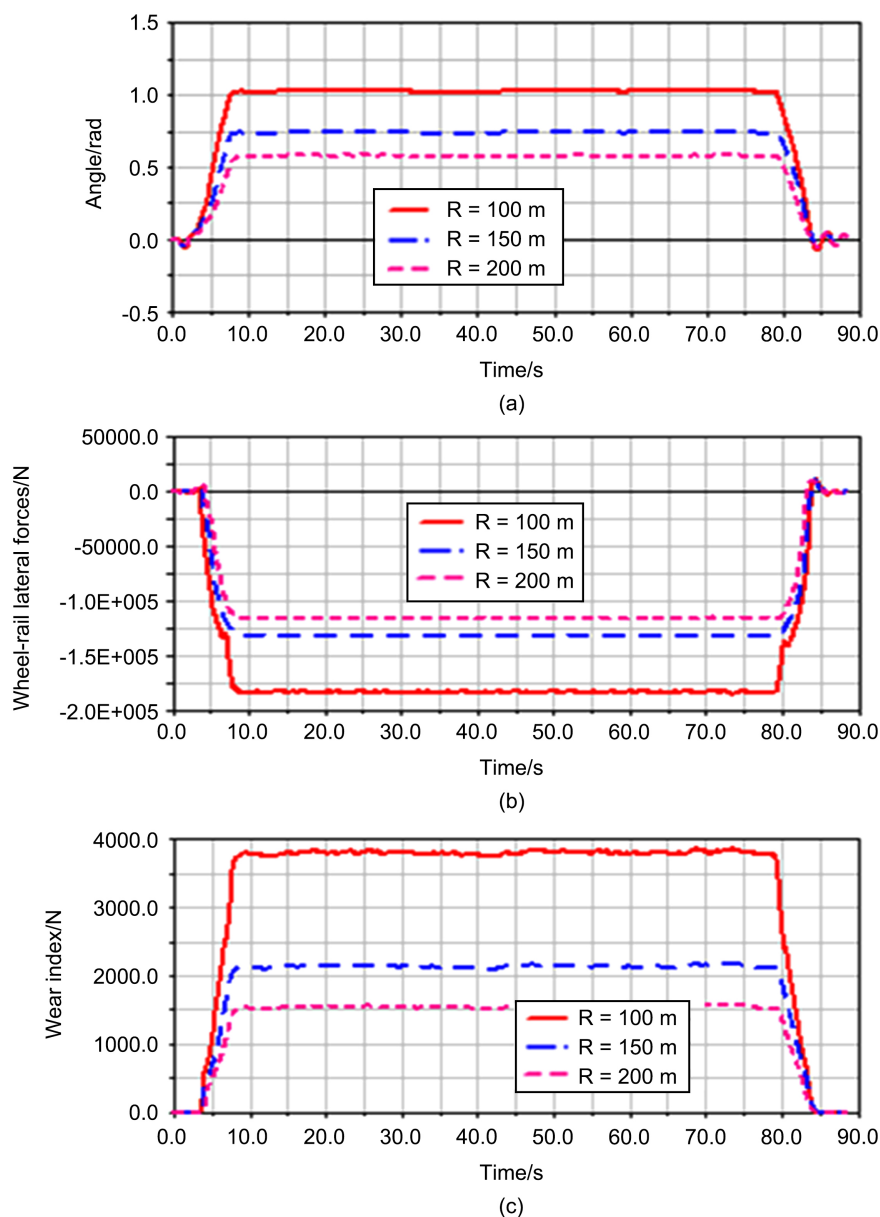


Figure 10. The effect of curve radius on wheel-rail wear. (a) Wheel-rail attack angle; (b) Wheel-rail lateral force; (c) Wheel-rail wear index.

The simulations showed that increasing the curve radius can effectively reduce wheel-rail wear of the vehicle system. Therefore, the curve radius should be increased if the workshop building area would permit it.

4.3. Operating Speed

The operating speed of a hot-metal car directly affects the efficiency of transporting molten iron. When the vehicle runs into curves, excessive speed will result in increased wear or even derailment. Operating speeds of 3.5, 4.0, and 4.5 m/s were respectively set as conditions 1, 2, and 3 to analyze the effect of different operating speeds on wheel-rail wear.

Figure 11 shows that the duration of attack angle, lateral force and wear index of the wheel-rail decreased with increasing speed, **Figure 11(a)** and **Figure 11(b)** showed that the trend of the wheel-rail attack angle was moderate changing.

Thus indicating that the effect of vehicle speed on the wheel-rail attack angle and wheel-rail lateral force was relatively small, whereas the wear index of the wheel-rail increased with increasing speed. Increasing speed resulted in more serious wheel-rail wear based on the simulation calculations.

4.4. Super-Elevation

The super-elevation is an orbital parameter. **Figure 12** shows that super-elevation had a negligible effect on the wheel-rail attack angle of the hot-metal car and had a

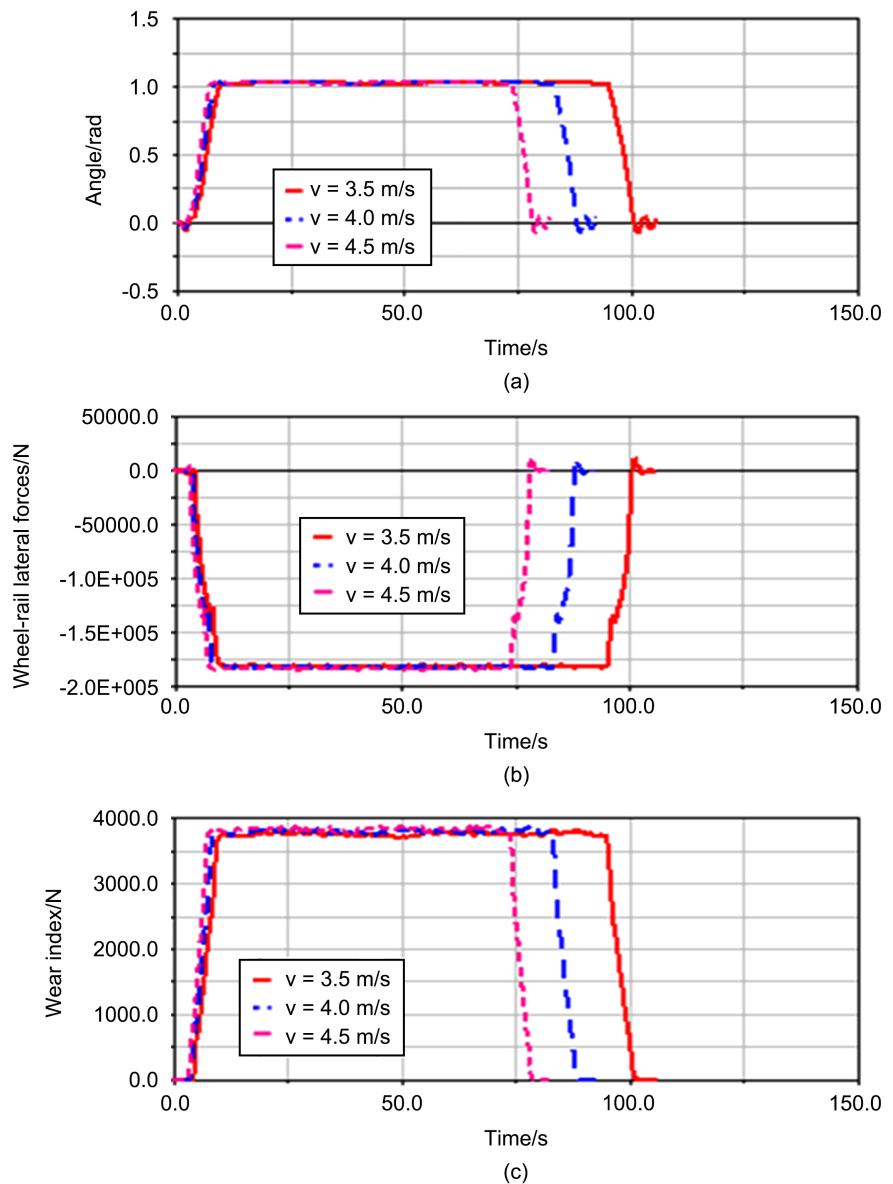


Figure 11. The effect of operating speed on wheel-rail wear. (a) Wheel-rail attack angle; (b) Wheel-rail lateral force; (c) Wheel-rail wear index.

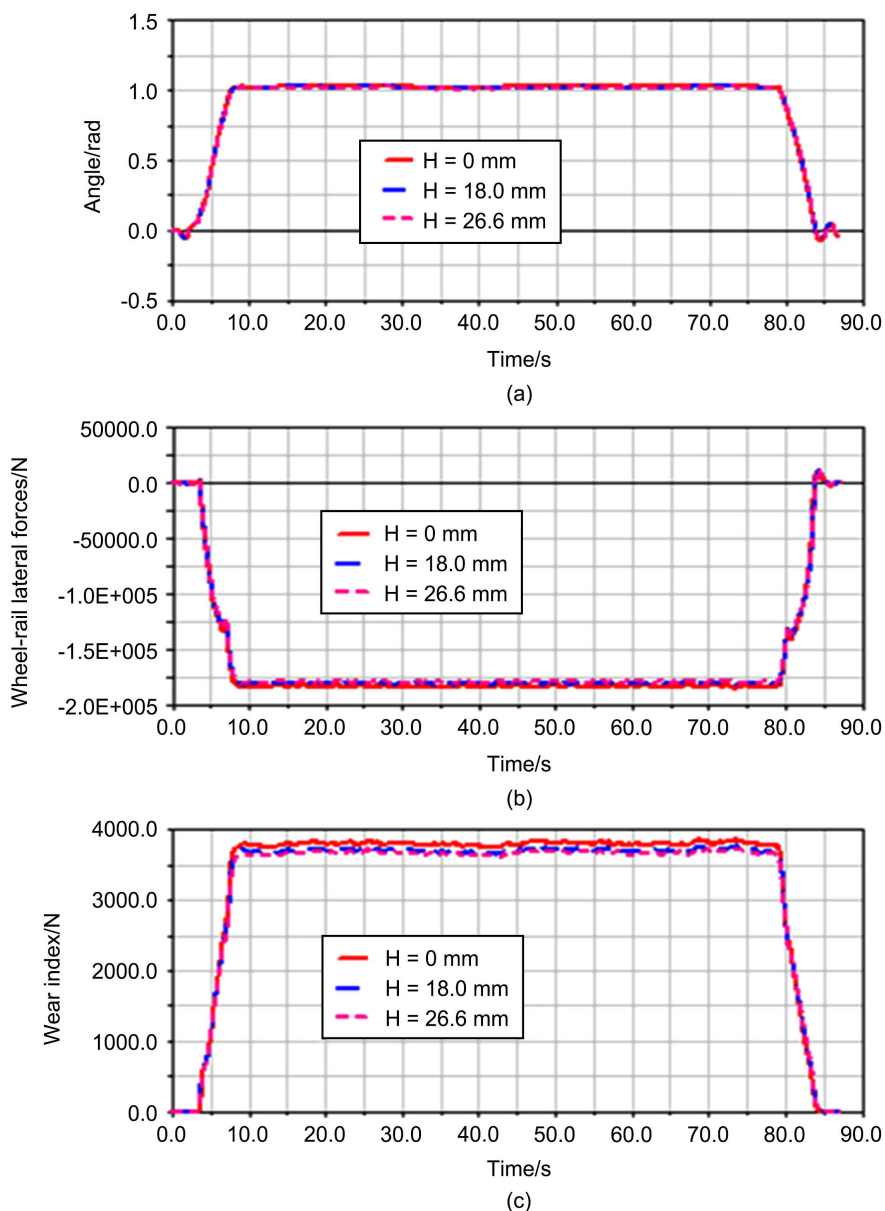


Figure 12. The effect of super-elevation on wheel-rail wear. (a) Wheel-rail attack angle; (b) Wheel-rail lateral force; (c) Wheel-rail wear index.

certain effect on wheel-rail lateral force. Lateral forces tend to decrease with increasing super-elevation, thus reducing the wear index of the wheel-rail. Based on this finding, an appropriate increase in super-elevation can reduce wheel-rail wear. A feasible option for manufacturers is to change existing curve lines.

5. Improvement Scheme for Reducing Wheel-Rail Wear

By considering the simulation result of the bogie and the relevant track parameters for wheel-rail wear, using the optimization tools of design of experiment in ADAMS facilitated the proposal of improvement measures, which include adopting a double-acting roller elastic side bearing, increasing the lateral and

longitudinal clearances of the side-frame box guide, and increasing curve super-elevation, etc. [15] [16] [17] [18] [19]. Experiment design may analyse the change of multi-design variable simultaneously. The change condition of objective function was studied when the value of these design variable was divided into groups according to different combinations. The proposed improvement scheme is shown in **Table 5**. The applied effect showed that the improvement scheme significantly affected various parameters of wheel-rail wear. The specific numerical values are listed in **Table 6**. The computational times is 205 seconds and the memory consumption is 25% of the new model in HPD03FS72 workstation.

Figure 13 shows the effect of the original and improved scheme on wheel-rail wear.

Table 6 shows that the maximum attack angle of the rear-wheel set decreased from the original 1.02 rad to 0.88 rad. Furthermore, the wheel-rail lateral force and wear index were evidently decreased after the improvement scheme was implemented, in which the wear index significantly decreased by 24.9% from the original 3820 N to 2870 N. These changes show that the improvement scheme effectively reduced the attack angle of the wheel set and obviously decreased wheel-rail wear. Moreover, the improvement scheme caused the derailment coefficient of the vehicle system, defined as the lateral force of the wheel divided by the vertical force of the wheel, to decrease by 5.7% from the original 0.601 to 0.567. The reduction rate of the wheel weight, defined as the reduction of the wheel weight divided by the wheel weight, decreased by 14.7%. These data show that the curving performance of the hot-metal car improved considerably.

Table 5. The comparison between original scheme and improvement scheme.

Scheme	Constant-contact elastic side bearing friction coefficient	Side frame box guide one side lateral clearance/mm	Side frame box guide one side vertical clearance/mm	Curve superelevation/mm
Original value	0.5	5	5	0
Optimized value	0.3	10	10	18

Table 6. The comparison of vehicle performance.

Scheme	Wheel set attack angle/rad	Wheel-rail lateral force/N	Wear index/N	Derailment coefficient	Reducing rate of the wheel weight
Original value	1.02	1.8e5	3820	0.601	0.85
Optimized Value	0.88	1.625e5	2870	0.567	0.73
Reduced rate/%	13.7	9.7	24.9	5.7	14.1

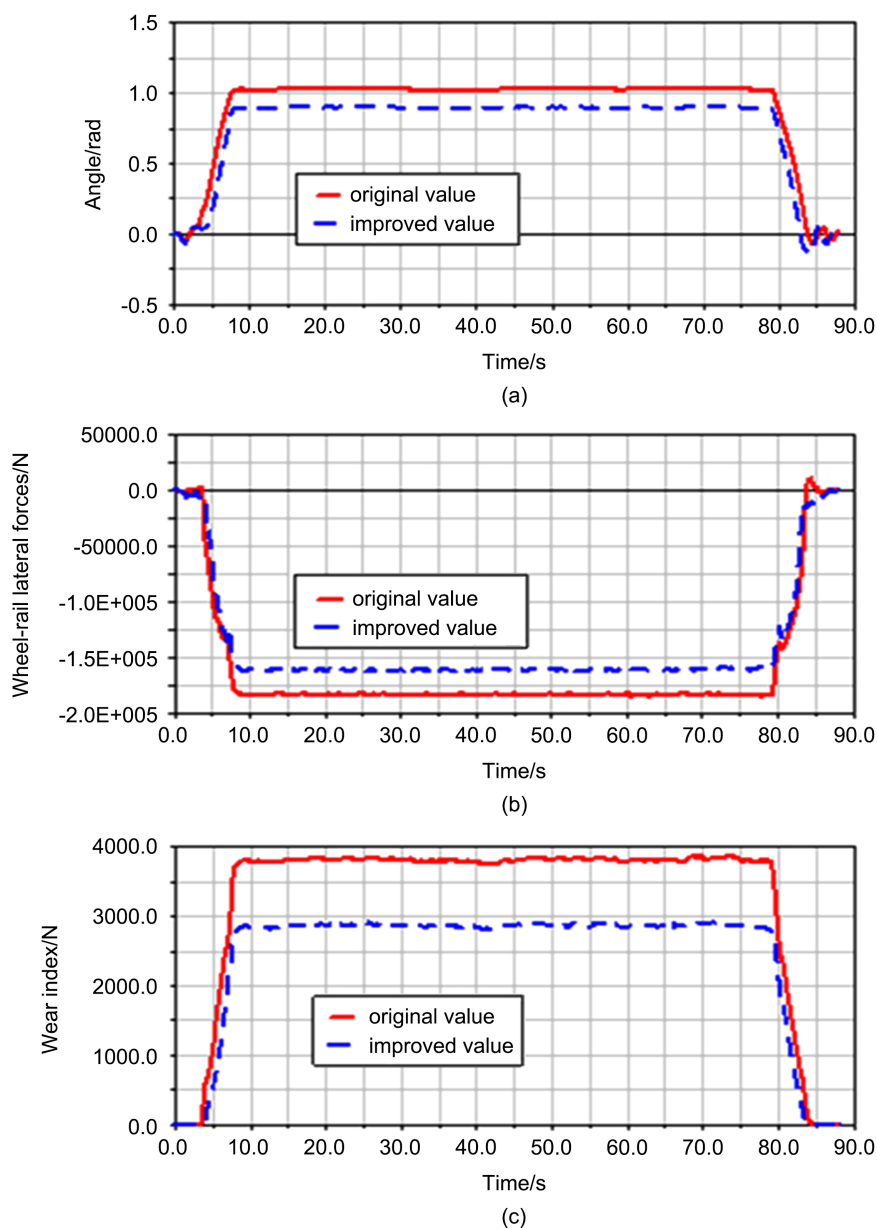


Figure 13. The effect of original and improved scheme on wheel-rail wear. (a) Wheel-rail attack angle; (b) Wheel-rail lateral force; (c) Wheel-rail wear index.

Moreover, when the vehicle ran on the circular curve, the vibration amplitude of the load reduction rate evidently decreased. This observation indicates that snake movement significantly weakened in the circular curve. Thus, the improvement scheme can effectively increase the curving performance of the vehicle system.

In addition, the simulation analysis showed that the top speed in the original scheme was 4.8 m/s (17.28 km/h), whereas the top speed reached 5.9 m/s (21.24 km/h) after the improvement scheme was applied. Such improvement in running speed can increase transport efficiency. After the improvement scheme is adopted, the vehicles manufactured are shown in **Figure 14**. The actual vehicle test was completed on the track with the curve super-elevation of 18 mm.



Figure 14. Adopted the improvement scheme vehicles manufactured.

6. Conclusions

1) In this study, the authors established the Pro/E model for a 140 t open-type hot-metal car. The rotational inertias of all components of the hot-metal car were calculated. The Pro/E model was imported into ADAMS/Rail to construct a dynamic model for the entire vehicle.

2) Through the simulation analysis of multiple dynamics, the effects of bogie and wheel-rail parameters on wheel wear were discussed. Among all the parameters of the bogie, the clearance of the side-frame box guide had a significant effect on wheel-rail wear. Spring vertical rigidity values, as well as the friction coefficients of the center plate and side bearing, had negligible effects on wheel-rail wear. Among all track parameters, curve radius was the most significant factor. Transition curve, running speed, and curve super-elevation all affected wheel-rail wear to a certain extent.

3) Based on the combined influence degrees of all parameters on wheel-rail wear the actual experience of the manufacturer, an improvement scheme for reducing the friction coefficient of the side bearing, as well as for increasing the clearance of the side-frame box guide and curve super-elevation, was proposed. The applied effect showed that the improvement scheme not only reduced wheel-rail wear and improved curving performance, but also increased top speed, which could increase the transportation efficiency of a hot-metal car.

Acknowledgements

This project was supported by the National Nature Science Fund of China (Grant No.11272220).

Conflicts of Interest

The authors declare no conflicts of interest regarding the publication of this paper.

References

- [1] Pipyuk, V.P., Polyakov, V.F. and Samokhvalov, S.E. (2009) Study of Hydrodynamics of a 350-Ton Ladle Bath during the Treatment of Steel on a Ladle-Furnace Unit. *Metallurgist*, **53**, 679-684. <https://doi.org/10.1007/s11015-010-9232-2>
- [2] Belkovskii, A.G. and Kats, Ya.L. (2009) Mathematical Model of the Cooling of Steel in Small Ladle. *Metallurgist*, **53**, 261-273. <https://doi.org/10.1007/s11015-009-9172-x>
- [3] Makarov, D.N., Gorbachev, Yu.P. and Andreev, V.A. (2007) Use of 140-Ton Ladle to Transport Liquid Pig Iron. *Metallurgist*, **51**, 486-488. <https://doi.org/10.1007/s11015-007-0086-1>
- [4] Ignesti, M., Malvezzi, M., Marini, L., Meli, E. and Rindi, A. (2012) Development of a Wear Model for the Prediction of Wheel and Rail Profile Evolution in Railway Systems. *Wear*, **284-285**, 1-17. <https://doi.org/10.1016/j.wear.2012.01.020>
- [5] Pombo, J., Ambrosio, J., Pereira, M., Lewis, R., Dwyer-Joyce, R., Ariaudo, C. and Kuka, N. (2010) A Study on Wear Evaluation of Railway Wheels Based on Multi-body Dynamics and Wear Computation. *Multibody System Dynamics*, **24**, 347-366. <https://doi.org/10.1007/s11044-010-9217-8>
- [6] Shabana, A.A., Zaazaa, K.E., Escalona, J.L. and Sanyc, J.R. (2004) Development of Elastic Force Model for Wheel/Rail Contact Problems. *Journal of Sound and Vibration*, **269**, 295-325. [https://doi.org/10.1016/S0022-460X\(03\)00074-9](https://doi.org/10.1016/S0022-460X(03)00074-9)
- [7] Meli, E., Falomi, S., Malvezzi, M. and Rindi, A. (2008) Determination of Wheel-Rail Contact Points with Semianalytic Methods. *Multibody System Dynamics*, **20**, 327-358.
- [8] Meli, E., Falomi, S., Malvezzi, M. and Rindi, A. (2005) Determination of Wheel-Rail Contact Points: Comparison between Classical and Neural Network Based Procedures. *Meccanica*, **44**, 661-686. <https://doi.org/10.1007/s11012-009-9202-6>
- [9] Xie, S.M., Yue, L.H. and Gao, Y. (2007) Based on Firm-Soft Mixture Model 300T Hot-Metal Car Dynamics Simulation. *Computer Simulation*, No. 24, 270-273.
- [10] Zhang, L.W., Li, F. and Huang, Y.H. (2009) Analysis on Special Molten Iron Tanker Curve Negotiation and Ride Performance. *Railway Locomotive and Car*, No. 29, 35-37.
- [11] Zhang, W.D., Mo, X.H. and Peng, J.S. (2007) Based on ADAMS the Hydraulic Plate Molten Iron Charter Dynamics Simulation. *Special Purpose Motor Vehicle*, No. 10, 35-38.
- [12] Zhai, W.M. (2012) Vehicle-Rail Coupling Dynamics. Science Press, Beijing.
- [13] Wang, C. (2011) Research on the Molten Iron Car Wheel Wear. Shijiazhuang Tiedao University, Shijiazhuang.
- [14] Yan, J.M. and Fu, M.H. (2012) Vehicle Engineering. China Railway Publishing House, Beijing.
- [15] Tao, G.Q., Wen, Z.F. and Guan, Q.H. (2003) Locomotive Wheel Wear Simulation in Complex Environment of Wheel-Rail Interface. *Wear*, **430-431**, 214-221. <https://doi.org/10.1016/j.wear.2019.05.012>
- [16] Ignesti, M. (2014) Development of a Model for the Simultaneous Analysis of Wheel and Rail Wear in Railway Systems. *Multibody System Dynamics*, **31**, 191-240. <https://doi.org/10.1007/s11044-013-9360-0>
- [17] Yang, G.X., Zhao, F.W. and Li, Q.Z. (2019) Study of Influences of High-Speed Train Wheel-Rail Contact Geometric Parameters on Wheel-Rail Wear. *Journal of the China Railway Society*, **41**, 50-56.

- [18] Wang, P., Wang, L. and Shabana, A.A. (2017) Influence of Rail Flexibility in a Wheel/Rail Wear Prediction Model. *Proceedings of the Institution of Mechanical Engineers, Part F: Journal of Rail and Rapid Transit*, **231**, 57-74. <https://doi.org/10.1177/0954409715618426>
- [19] Magel, E. and Kalousek, J. (2017) Designing and Assessing Wheel/Rail Profiles for Improved Rolling Contact Fatigue and Wear Performance. *Engineers Part F Journal of Rail and Rapid Transit*, **231**, 805-818. <https://doi.org/10.1177/0954409717708079>